Journal of Engineering and Sustainable Development
Vol. 30, No. 03, May 2026
https://jeasd.uomustansiriyah.edu.iq/index.php/jeasd
ISSN 2520-0917
Research Article
https://doi.org/10.31272/jeasd.2452

Experimental Study to Evaluate the Load-Bearing Capacity of Autoclaved Aerated Concrete Block Walls

Sarra'a Dhiya'a Jaafer, Ashraf A. Alfeehan*

Civil Engineering Department, College of Engineering, Mustansiriyah University, Baghdad, Iraq.

*Email: drce_ashrafalfeehan@uomustansiriyah.edu.iq

Article Info

Received	07/02/2024
Revised	04/04/2026
Accepted	16/04/2026

Abstract

It is common to use Autoclaved Aerated Concrete (AAC) blocks in the construction of partition walls and infills because of their distinctive properties, including ease of work, energy conservation, and enhanced sustainability. Experiments for the strength evaluation of AAC load-bearing walls are still limited. This paper presents an experimental study of the behavior of AAC blocks as load-bearing walls under static loads up to failure. Due to the difficulty of using the direct contact method to measure and monitor deformations in walls, the Digital Image Correlation (DIC) method was used to obtain the required data throughout the test. Eight specimens of confined walls were tested to study the effect of the thickness of the block, type of bonding material, and type of plastering on the wall strength and failure modes. The results showed that the smaller the thickness of the AAC block, the greater the strength of the wall. Also, using adhesive mortar leads to the cohesion of the wall and increases its load-bearing capacity better than using cement-sand or gypsum mortar. In addition, strengthening the plastering with steel wire meshes showed superior performance in wall behavior in improving cracking resistance and ultimate loads.

Keywords: Autoclave Aerated Concrete; Bearing Wall; Confined Masonry; Digital Image Correlation; Mortar and Plastering Material

1. Introduction

Masonry is generally used for the construction of load-bearing walls and infill walls. Autoclaved Aerated Concrete (AAC) is one of the building units; it's a lightweight building material used broadly in constructions as bearing and non-bearing walls. Using AAC masonry as a bearing wall has many advantages, such as lightness, fine thermal protection behavior, excellent fire resistance, convenience for construction, and environmental friendliness. AAC block walls can effectively offer thermal insulation, lightness, and workability solutions for structural masonry and infill panels [1]-[7]. The AAC block is used worldwide because of its deformability and low weight, reducing the inertia force [8], [9]. It is necessary to promote the development of green buildings, and there is great concern and emphasis on lowering greenhouse gas emissions in the air to control adverse environmental effects, also its small weight makes it easier to move around on the construction site and provides better thermal insulation for cozy conditions [7], [10]-[12], AAC is sufficient to be used as a construction material in low-rise structures, and it's used in seismic regions and multi-story residential building because the use of AAC leads to a reduction in seismic inertia forces can reduce the building weight and improves the seismic behavior thanks to its low-density because the AAC blocks have smaller volume density and homogenous [13], [14]. AAC blocks are strong under compression but weak under strain, and cracks spread quickly on the masonry structure's surface because of the low ductility. For that, the blocks must meet the minimum strength requirements specified in the standard for their usage in walls before being used as a building material [15].

J. Yu et al. studied and analyzed the failure features and shear strength of the walls of the AAC block wall due to different h/w ratios and vertical pressing stress. Also, studied the deformation behavior and dissipative capacity of the walls, and concluded that the h/w ratio and vertical pressing stress had a great influence on the failure feature of the AAC load-bearing block wall, and the ductility of AAC block walls is better than other block walls [16], [17]. Bhosale et al investigated some of the physical properties of AAC blocks that influence the structural properties and overall behavior of AAC masonry [18], [19].

Confined masonry carries a portion of the vertical load. For confined masonry, the process in which the structural parts are erected is particularly significant. In addition to being performed as reinforced masonry [20], confined masonry is an acceptable alternative for improving the design resistance [20],

[21]. Also, AAC masonry blocks have been an attractive solution during the last decades for the construction of walls due to their advantages [21]. Drobiec et al analyzed the load-bearing capacity and deformability of AAC walls as confined and unconfined walls with filled and unfilled perpend joints were made [22].

A significant effort has been devoted in previous research to studying the behavior of AAC walls under some parameters, but it did not clarify the full behavior of AAC walls as bearing walls. Therefore, there is an urgent need to define design criteria for using AAC walls as bearing walls. The significance of this work is that it provides a clearer picture of the employment of AAC blocks in the construction of load-bearing walls under higher loads in an attempt to remove doubt about this issue, as well as giving an engineering recommendation for constructing buildings using AAC safely.

The study aims to conduct practical tests on the properties of building AAC blocks and the materials used to bond and plaster the blocks, and then give a complete understanding of the behavior of AAC walls as load-bearing structural walls under static loads. The work covers a study of the influence of several variables, such as the thickness of the AAC block, the type of bonding materials, and plastering layers on the wall's bearing capacity and its structural performance by observing the cracking loads, ultimate loads, and failure modes. To attain this aim, a proper non-contact technique for wall testing called digital image correlation DIC was applied.

2. Materials and Methods

2. 1Material

The dimensions of the AAC block used in this work were 600 mm in length, and 200 mm in thickness, but differ in height to (100,150 and 200) mm. Three types of mortar were used to bond the AAC blocks: cement-sand mortar, gypsum mortar, and adhesive mortar, which is considered today a commonly used material as a bonding material for AAC blocks. The volumetric ratio of cement-sand mortar is 1:3, and the w/c is 0.6. Portland ordinary cement and natural sand as a fine aggregate were used throughout the work. Mesh reinforcement was used to assist in maintaining plaster integrity and minimizing consequential cracking. Galvanized steel square wire mesh was used to reinforce the plastering layer. The dimensions of a mesh opening were (20×20) mm with a 0.5 mm diameter of the wire. The values of the mechanical properties tests that were conducted for the above materials are tabulated in Table 1. The test results of the steel wire mesh are listed in Table 2.

Table 1. Mechanical Properties of Material

Property	Value			
	AAC Block	Cement-Sand Mortar	Gypsum Mortar	Adhesive Mortar
Density (Kg/m^3)	585	2071.7	1880	1560
$f_c^{'}$(MPa)	2.2	18.5	5.2	9.4
f_t (MPa)	0.116	1.87	1.42	3.25
f_r (MPa)	0.36	2.3	0.78	1.28
E_c (MPa)	438.7	3400	1100	1400
ν	0.168	0.227	0.17	0.182

Table 2. Test Results of Steel Wire Mesh

Normal Diameter (mm)	Yield Stress MPa	Ultimate Strength MPa	Elongation %
0.5	1395.55	1725.37	8.8

2.2. Experimental Work

The experimental work includes first manufacturing the supporting test frame, and building specimens of the AAC walls inside the frame, testing them, and observing the structural behavior using the digital image correlation technique.

2.2.1. Supporting Frame

To conduct testing on AAC walls and approximate the specimens to the reality of construction, a steel structure was manufactured in which the wall was built and tested within fixed boundaries. All the walls were tested under a static load distributed on the top bearing surface to investigate their structural behavior. The load was applied by a hydraulic jack with a capacity of 100 tons, which is installed on the top of the structure from the inside. The jack was equipped with a manual hammer and a measuring watch. The steel frame was designed to resist vertical loads only, and at the bottom, it rests on a steel plate supported on the ground, but from above, a steel beam with higher strength than the wall and the jack was used. The closed steel frame was designed to resist the high compressive forces resulting from the applied load while providing a confined field for the wall on all sides. The frame was made of steel section C (240×80×7) mm with a length of 1600 mm for the base and a pair of vertical columns of 1900 mm each. A steel box beam was welded on the top of the frame, resting on both columns at both ends. The steel box beam was made up of an H section (250×250) mm, t_w=9 mm, and t_f=14 mm and thickened on all sides by an 8 mm steel plate that was fixed by welding. A steel loading plate of 22 mm in thickness was suspended by four springs from the bottom of the steel box beam to spread the load on the wall uniformly. The steel loading plate was a rectangular section, with dimensions (1160×220×22) mm. A 20-mm-thick pad layer of high-density rubber was placed between the loading plate and the wall surface to ensure load distribution and prevent concentrated loads at specific areas. The steel frame was provided with four wheels to facilitate movement, and the wheels were removed during the test. The fabricated steel frame is shown in Fig.1.

Figure 1. Confined Wall in Steel Frame.

2.2.2. AAC Wall Specimens

Eight specimens of confined walls with dimensions (1200×1200×200) mm were tested to study the effect of the thickness of the block, type of bonding material, and type of plastering on the wall resistance and failure modes. To study the effect of the variables individually, the specimens were divided into three groups. The first group included three walls in which the thickness of the blocks varied between 100, 150, and 200 mm as shown in Fig. 2. As for the second group, it also included three walls, and a different type of bed bonding material was used for each wall; cement-sand, gypsum, and adhesive mortar, while the third group included two walls that were plastered with cement-sand mortar on one side and gypsum mortar on the other side, with the face of the cement-sand mortar reinforced with wire mesh for one of the two walls. The thickness of the bonding layer was 10 mm for cement-sand and gypsum material, whereas it was about 3 mm for adhesive mortar according to the specification.

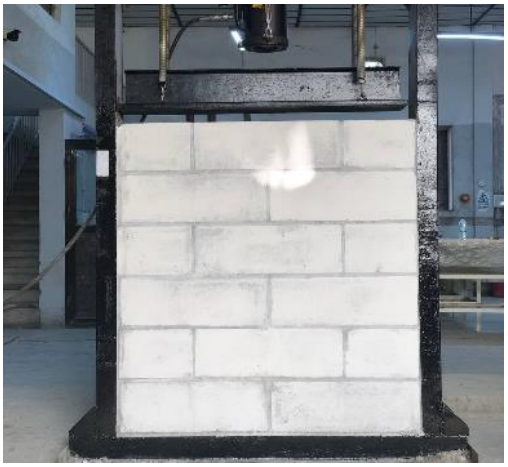

(a) 200 mm

(b) 150 mm

(c) 100 mm

Figure 2. ACC Block Courses (100,150 and 200 Thickness)

2.2.3. Wall Testing

Before starting to apply the load to the wall, it is prepared for digital imaging by drawing a network of points over the entire surface of the wall. The camera is then placed in a fixed location suitable for taking clear pictures during the loading steps. The load is applied by a hydraulic jack mounted on top of the supporting frame and connected to a hand hammer with a rubber hose, as shown in Fig. 3. This process continues until the first crack (P_{cr}) and the final failure appears (P_u).

Digital Image Correlation (DIC) uses particle images to measure flow speed. The method of DIC measures a point velocity by following a texture patch, shown in the primary digital image, by a digital image series [20], [23]. Every patch has a unique texture and particular coordinates in image 1 at time = (u1, v1). To determine the coordinates of the patch from

image 1 within the search area of the larger patch that previously corresponded to image 2, the

Figure 3. Wall Test.

A relationship was evaluated between the two patches. The highest correlation with a location inside the patch research shows particular coordinates of the primary patch at time = in image 2, as appeared in Fig.4, repeated process inside the image for a whole mesh of patches after that is repeated for all images inside the series, to locate the vector of displacement in every test patch [23], [24].

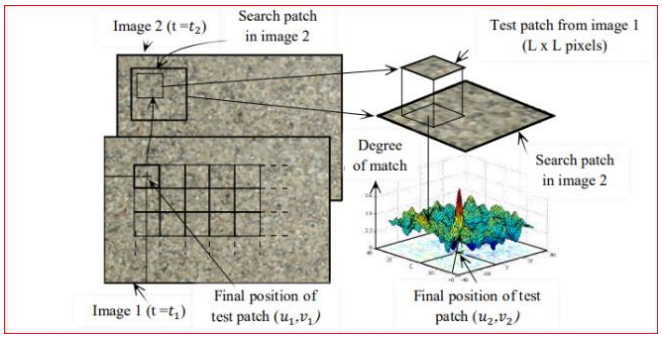

Figure 4. Principle of DIC Analysis.

The DIC technique is more appropriate for analyzing the nonlinear behavior of masonry structures because of its full-field capability, which yields reasonably accurate data regarding deformation, micro-cracking, crack propagation, and stress concentration locations. Therefore, in the present study, the walls are painted white, and they have been spotted with black paint with distances between spots of 20 mm center to center vertically and horizontally. In this research, the DIC system has been used to calculate and analyze full-field deformations of walls under static loads and strain distribution of tested walls by using the viscoelastic analysis for the tested walls using the GOM Correlate Pro software program version 2022. A digital camera has been used with a picture size of 3648×2736 (10M) pixels and an aspect ratio of 4:3 for the documentation of specimen reaction.

3. Results and Discussion

Based on the provisions of the 2008 MSJC Code and Specification for design AAC masonry elements, which calculates the bearing wall stress equal to:

$$0.6 \times 0.85 \times f'_{AAC} \quad (1)$$

where, f'_{AAC} is the compressive strength for AAC block.

The equation results together with the experimental results of the first crack load (P_{cr}) and ultimate load (P_u) are summarized in Table 3. The equation result is 1.21 MPa, showing acceptable convergence for non-plastered walls, while the experimental results were higher than the equation results for plastered walls, which shows the effect of these variables that were not taken into account in the equation.

AAC block material is considered a brittle material with little elasticity and a weak ability to withstand tensile and bending stresses, but this behavior may differ slightly when the blocks are built together and plastered with external and internal mortar, as the blocks are confined within an external and internal mortar shell, and their behavior becomes similar to that of sandwich panels under axial loads.

In general, after the application of loads, at low load levels, the AAC walls behaved elastically. Where no cracks appeared, and the deformation is very small at the wall, because the stress at this stage is still small, and the wall could resist the applied load. When the load is increased, almost at a load level between (35-41) % of the ultimate load, the first cracks appear in the blocks under the loading zone because of the high compressive stress in this zone. After that, some inclined and horizontal cracks grow in the blocks in the position of the confinement, and the crack width is increased, and other inclined cracks appeared on both faces of the walls till the load reached the ultimate level.

After the failure, the walls appeared with some crushing in blocks. Some failure patterns observed were typical in almost all walls, which predicts an initially linear elastic behavior followed by the initiation and progression of damage. After cracking, there is a decrease in stiffness during the post-elastic phase, although the joints can still transmit force. With the bearing capacity dropped and the displacement increased, the main cracks further developed, and lots of secondary cracks were formed. At last, the major crack and several of the crushers had caused damage to the wall, as shown in Fig 5. The maximum load had been used to finish this phase.

Cracks appear in walls for several reasons, and by eliminating the cracks resulting from the foundation settlement in this case study, the cracks appear as a result of high loads that cause mainly compressive stresses in addition to shear stresses. Cracks spread on the wall surface and move from the weak to the strong material, depending on the confinement conditions and the air gaps that exist between the different materials and the same material.

All walls were kept equal in dimensions, but there is a slight difference in the dimensions of some walls due to the change in the number of horizontal mortar layers, depending on the thickness of the AAC block or due to the presence of vertical mortar.

It is generally clear from the results that the bearing stresses of the walls under cracking loads, which in turn are higher than service loads, and under ultimate loads, are also less than the AAC block strength. It is noted that models W7 and W8 bear ultimate stresses higher than the strength of the AAC blocks. When the block height was reduced from 200 mm to 150 mm, the first cracking and ultimate loads increased by approximately 15% and 20%, respectively. As the height reduced from 200 mm to 100 mm, the first cracking and ultimate loads increased by 43% and 47%, respectively.

Table 3. Results of Tested Walls.

Group	Wall	Block Thickness mm	Bond Material	Mortar Direction	Plastering	P_{cr} (kN)	P_u (kN)	Ultimate Stress (MPa)	Exp/Eq.1
1	W_1	200	Cement-sand	H	-	115	299	1.25	1.03
	W_2	150	Cement-sand	H	-	132	358.6	1.49	1.23
	W_3	100	Cement-sand	H	-	164	440	1.83	1.51
	W_4	200	Cement-sand	V & H	-	146	359	1.47	1.21
2	W_5	200	Gypsum	V & H	-	119.5	343.6	1.41	1.16
	W_6	200	Adhesive	V & H	-	202	508	2.08	1.72
	W_7	200	Adhesive	V & H	Cement-sand + gypsum	270	760	3.1	2.56
3	W_8	200	Adhesive	V & H	Reinforced cement-sand + gypsum	299	865	3.5	2.89

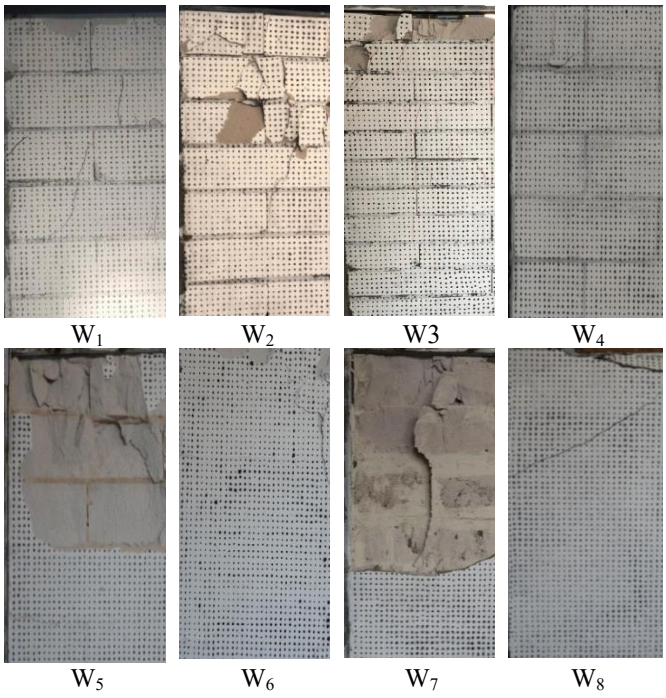

Figure 5. Failure Patterns for Wall.

The increase in the first crack and ultimate loads of the wall with the decrease in the thickness of the block unit is due to the increase in the number of strong mortar layers relative to the thickness of the AAC block layers. The decrease in the thickness of the AAC blocks reduces the formation and growth of vertical and inclined cracks in the AAC layers, and the mortar begins to act as a barrier for these cracks because of its high compressive strength, which leads to an improvement in the wall's overall strength.

When gypsum mortar was used in vertical and horizontal bonding mortar, the first crack and ultimate loads were reduced by 18% and 4%, respectively, while the loads increased when using adhesive mortar by 38% and 41%, respectively, compared to the cement-sand mortar. This is because cement mortar has a higher strength than gypsum mortar, resulting in the presence of layers that can withstand compressive forces between the building blocks, whereas the use of adhesive mortar leads to increased cohesion of the AAC building units vertically and horizontally and improves the bearing capacity of the wall.

Placing layers of cement-sand mortar on one side and gypsum mortar on the other side as plastering layers on the faces of the walls led to an improvement in the cracking load and the ultimate load. The loads increased by 34% and 50%, respectively, while the increase was by 48% and 70%, respectively, when the cement-sand mortar was reinforced with wire mesh compared to a wall without plastering layers. It is clear that placing layers of plaster leads to an increase in the surface tensile strength on the face of the wall and also contributes to resisting loads through an increase in the section of the wall. This results in preventing or delaying the occurrence of cracks and crushing in the AAC units, and the behavior of the wall is similar to the behavior of sandwich panels, which leads to an increase in the stiffness of the wall and its endurance.

The aims of determining the strain for all the tested walls were to obtain the maximum compressive and tensile strain and their locations, and also to indicate the formation of the initial cracks. As shown in Fig.6, the x-axis of the curves represents the number of photos that were taken through the test by the DIC technique, and also represents the loading step, where the y-axis represents the strain values. Also, the indicated points refer to

the higher values of strains that are calculated automatically by the program; the red points indicate the highest positive reading of strain (compression), while the blue points indicate the highest negative reading of strain (tension), and the color gradient on the right of the pictures in Fig.6 illustrates this. At the early stage of loading, the development of strains is very small. The increase in the load occurs due to a sudden change in the strain values; at this stage, the first crack appears and takes place. After that, the strains increased with any loading increase, and the cracks appeared on the wall surface. It's clear from the curves below that after the strain reached the ultimate strain, the cracks began to form and widen, due to the higher stress in the mortar and AAC blocks.

Table 4 shows the tensile and compressive strains at ultimate load in both directions calculated by the GOM program. Positive deformations in walls W7 and W8 indicate that the plaster layer separates from the wall and shatters in some locations because the spots were painted on the plastering layer, not on the block. The deformation is read for the plastering layer in the z-direction because of the separation. As a result, at high loads, an opposing displacement occurs between the AAC blocks and the plaster layer.

The deflections resulting from the applied loads are deformations within the walls due to the confined state of the walls during the test. These deformations are affected by several factors, the most important of which are the presence of voids in the bonding mortar, the weak strength of the mortar, or the occurrence of cracks and crushing in the AAC blocks. When comparing these deformations under equal loads for the walls in each group, it appears that the deformations are less when using a larger thickness of the block in W1, which in turn reduces the number of layers of bonding mortar between the rows of the wall, as shown in Fig. 7. Also, the use of different types of bonding mortar showed that deformations are higher in walls with cement-sand mortar W4 compared to other types under approximately the same load. Due to the high resistance of the cement-sand mortar, deformations are transmitted to the AAC blocks, giving higher values, as shown in Fig. 8. Using a plastering layer on the wall, the deformations are first read on the plastering layer. The wall W8, in which the plastering layer was with steel wire mesh, showed lower deformation values than the wall without wire mesh under equal load values. This is attributed to the increased contribution of the wire mesh in resisting cracks and providing higher bonding forces with the wall surface, as in Fig. 9.

Table 4. Results of Ultimate Strains by DIC Technique.

Wall	X-Strain $\times 10^{-3}$		Y-Strain $\times 10^{-3}$		Y-Ultimate Deformation (mm)	Ultimate Load (kN)
	Comp +	Ten -	Comp +	Ten -		
W_1	14.6	6.44	17	14.4	-4.6	299
W_2	10.1	6.2	12.7	11.9	-15.3	358.6
W_3	13.5	11.7	14.9	12.3	-12.9	440.3
W_4	6.06	5	11.4	11.1	-4.1	359
W_5	11.3	13.1	12.7	20.9	-15.8	343.6
W_6	16	12.3	16.2	16.9	-9.1	508
W_7	11.53	3.4	14.4	7.9	+11.76	760
W_8	6.3	9.6	5	5.5	+7.8	865

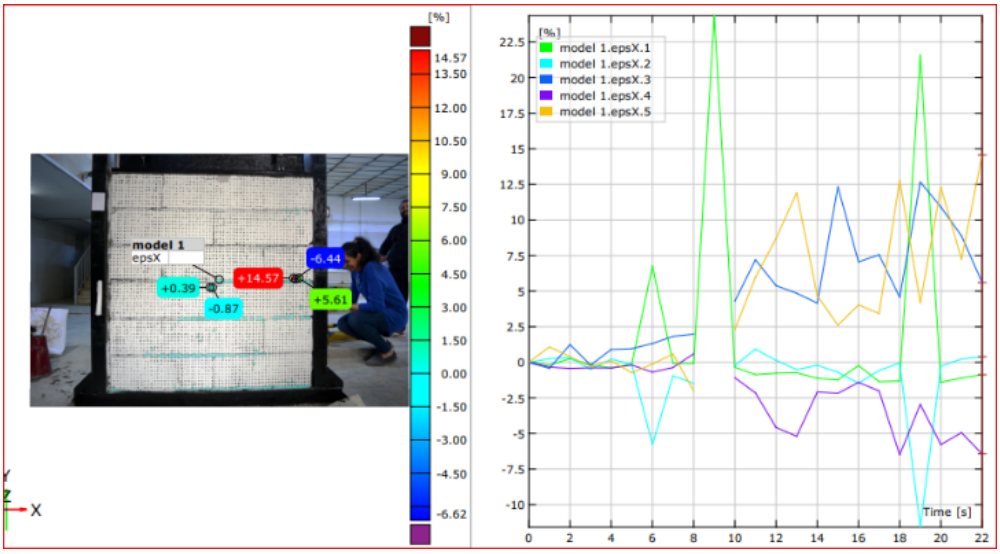

(a) X-Strain for W1.

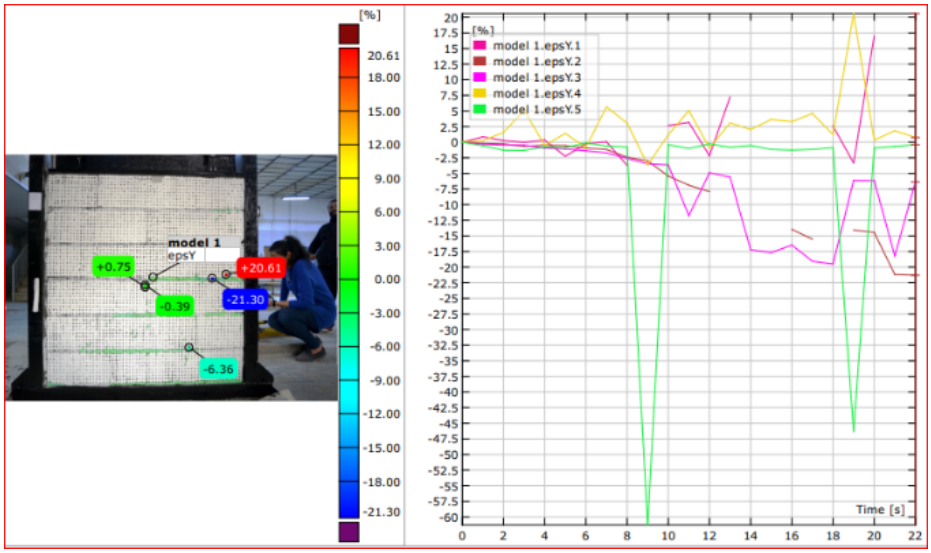

(b) Y-Strain for W1.

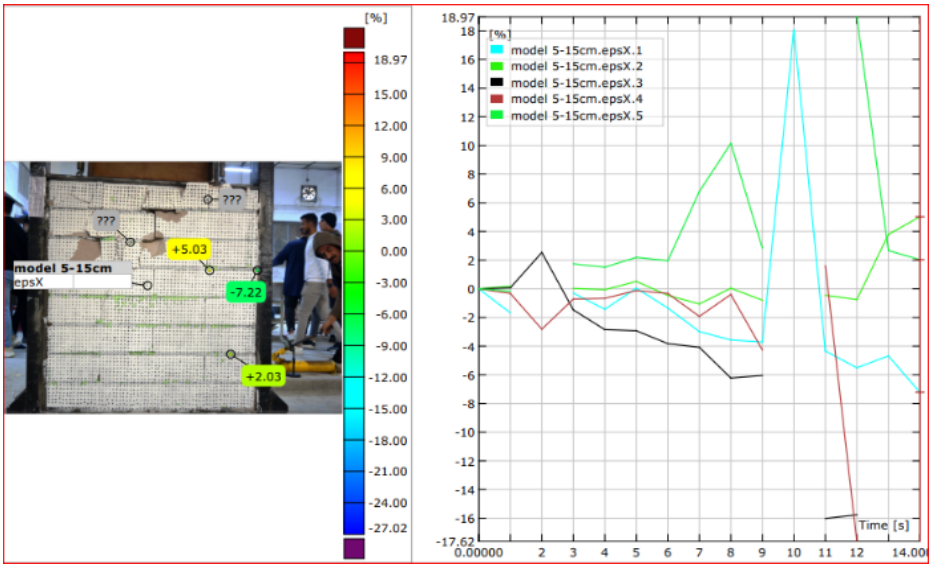

(c) X-Strain for W2.

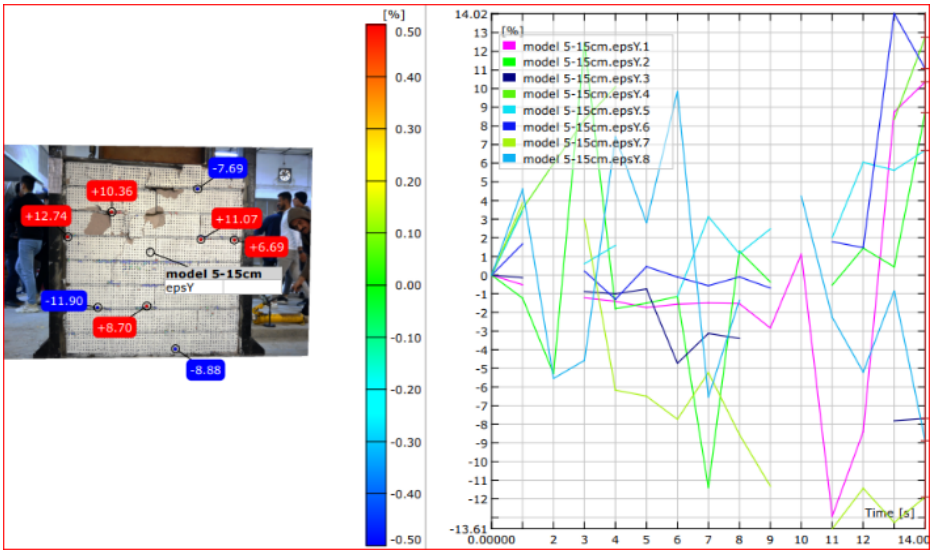

(d) Y-Strain for W2.

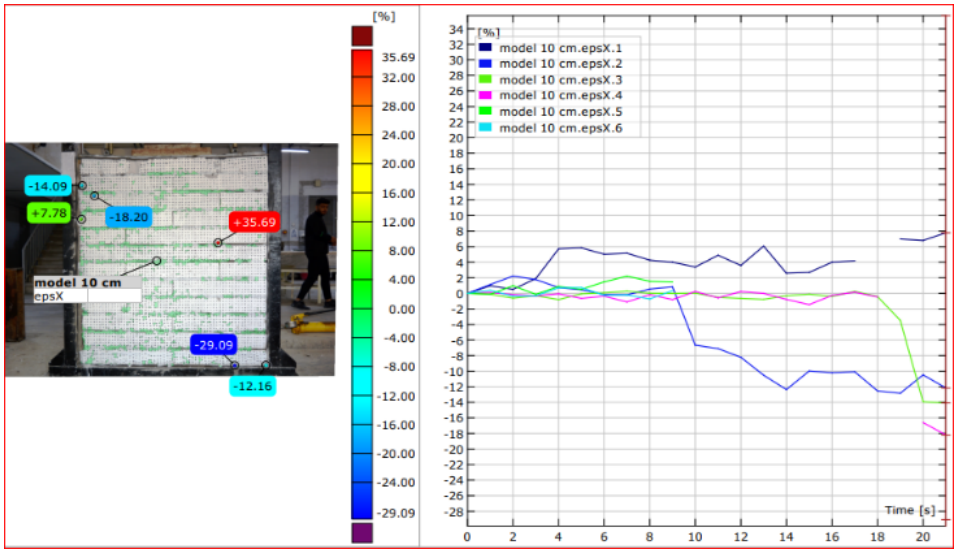

(e) X-Strain for W3.

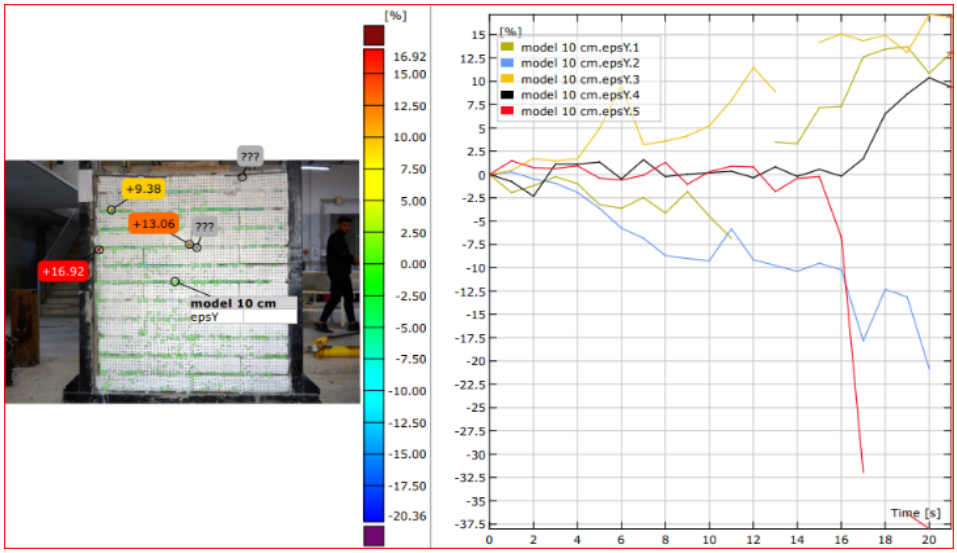

(f) Y-Strain for W3.

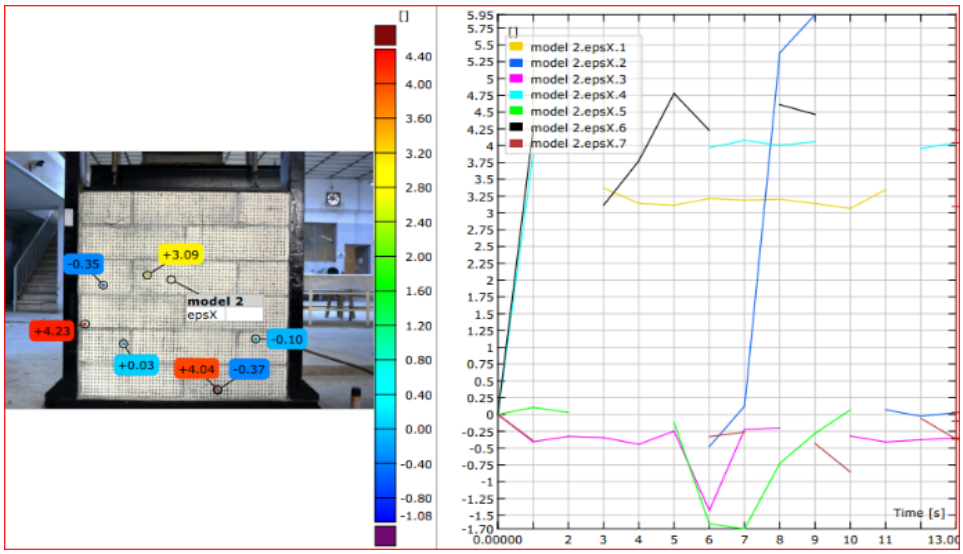

(g) X-Strain for W4.

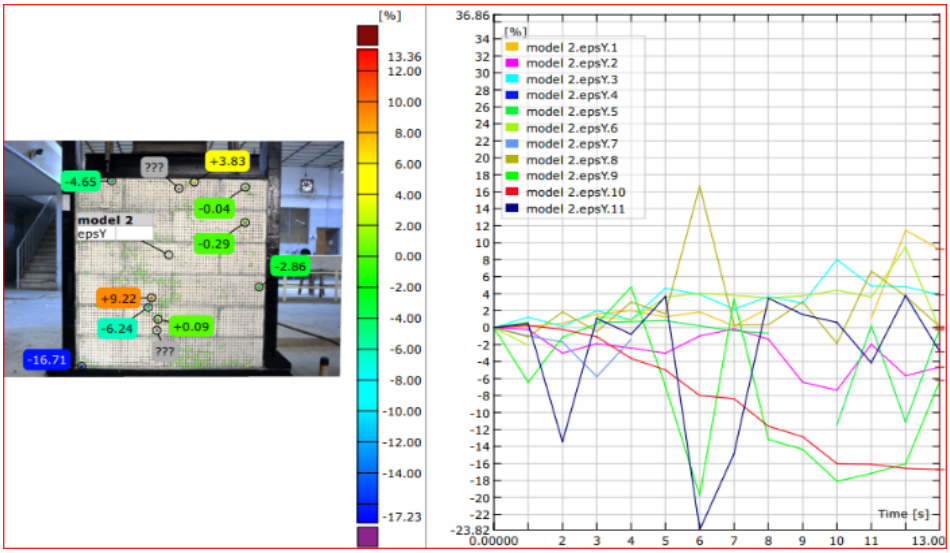

(h) Y-Strain for W4.

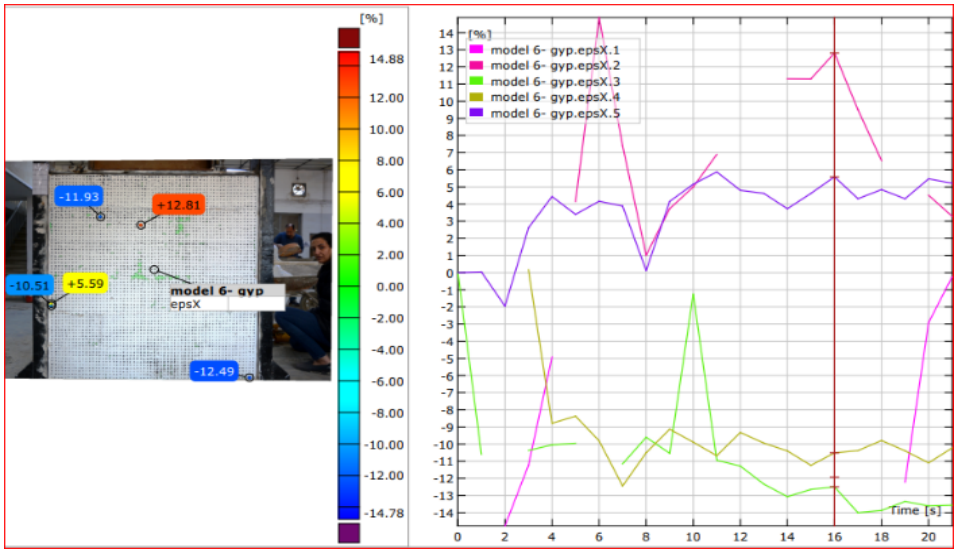

(i) X-Strain for W5.

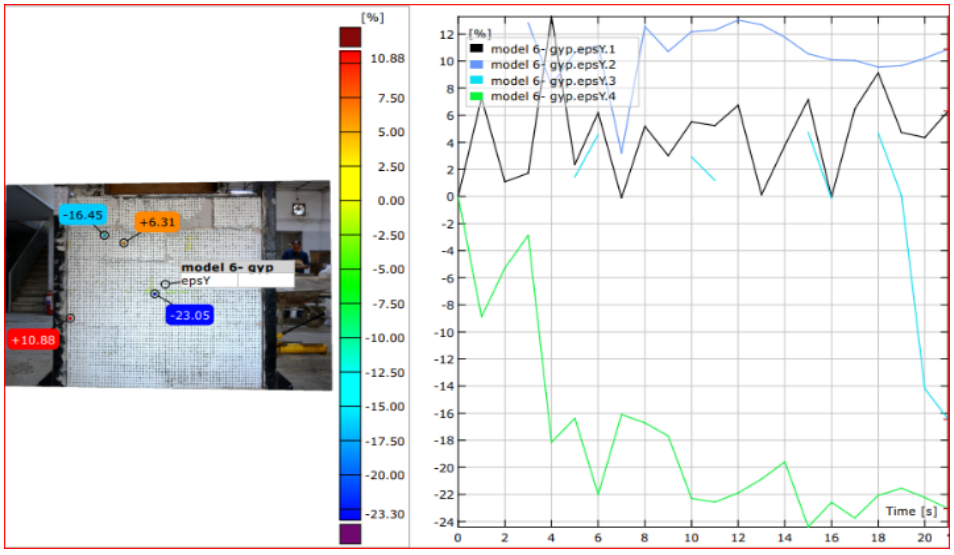

(j) Y-Strain for W5.

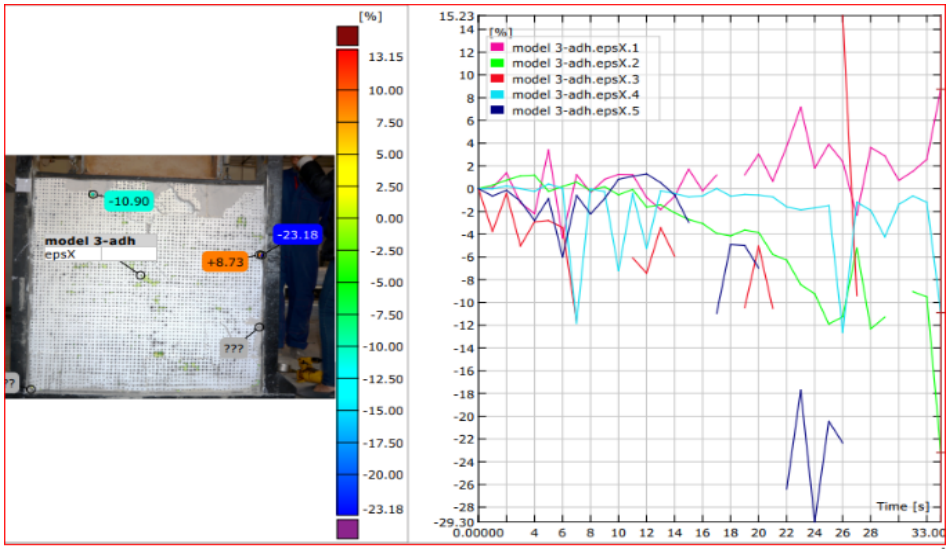

(k) X-Strain for W6.

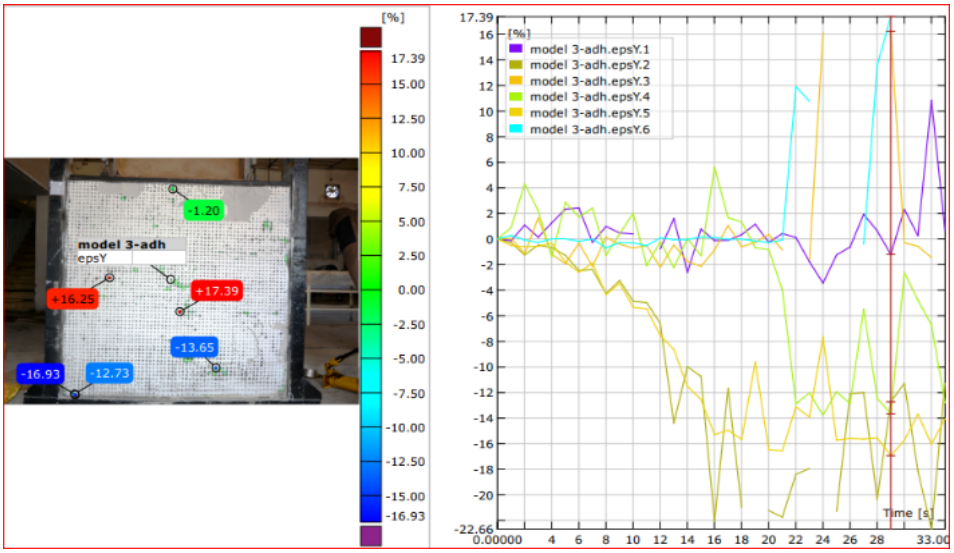

(l) Y-Strain for W6.

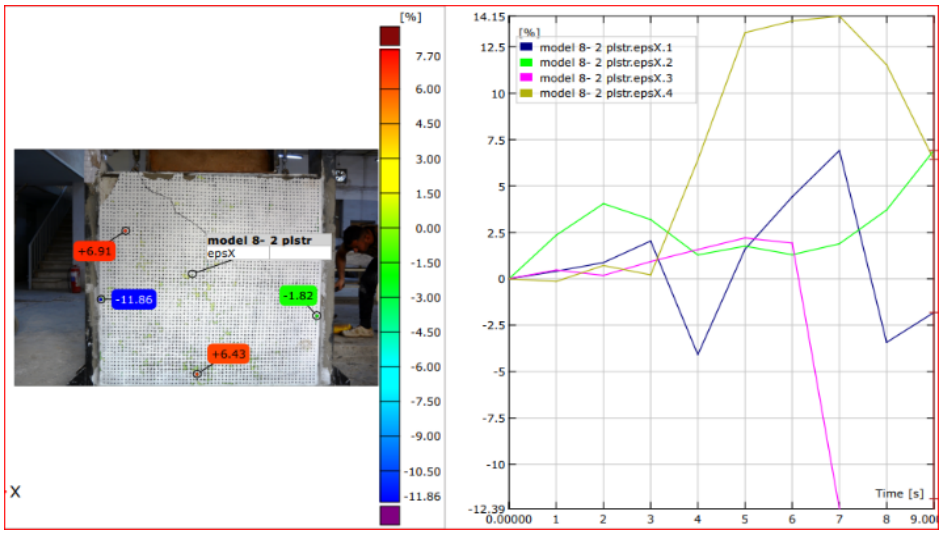

(m) X-Strain for W7.

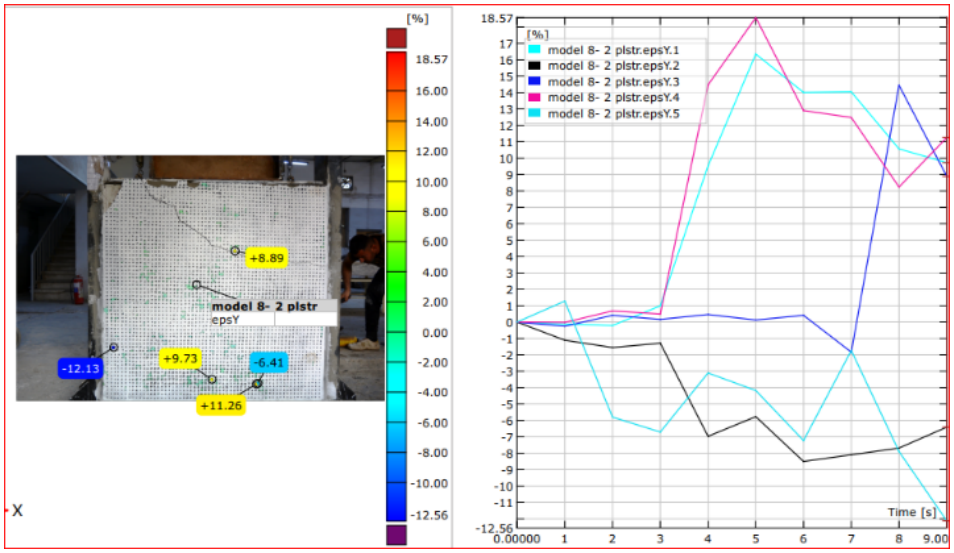

(n) Y-Strain for W7.

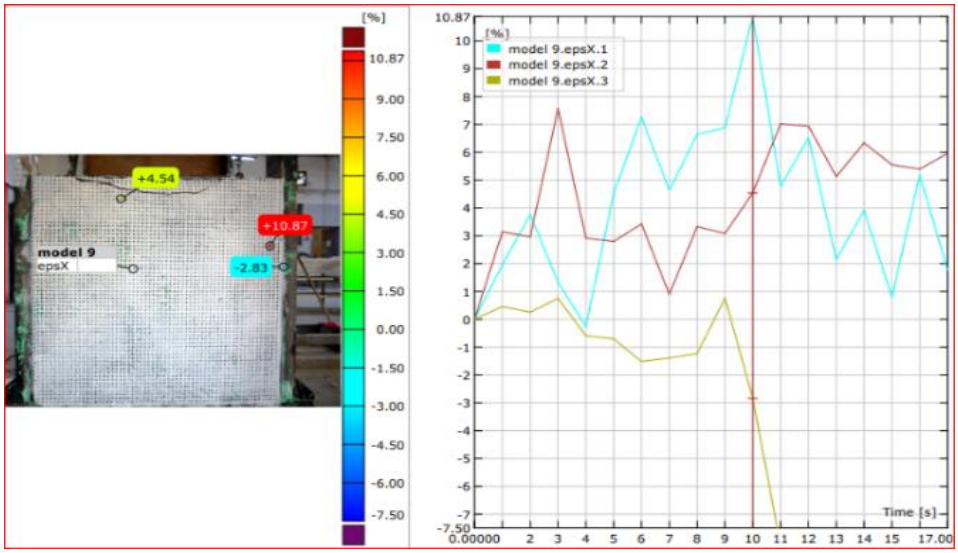

(o) X-Strain for W8.

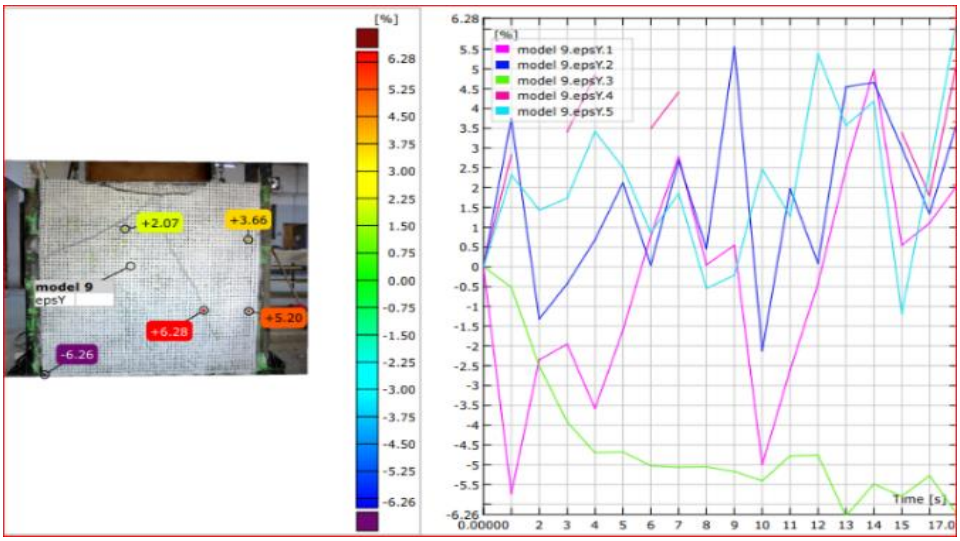

(p) X-Strain for W8.

Figure 6. Strains of Walls.

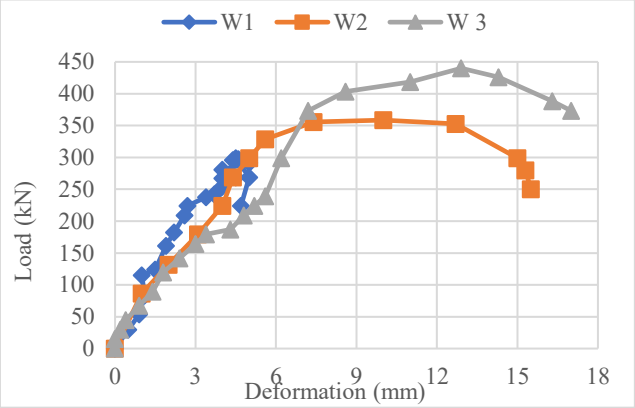

Figure 7. Load-Deflection of Group 1.

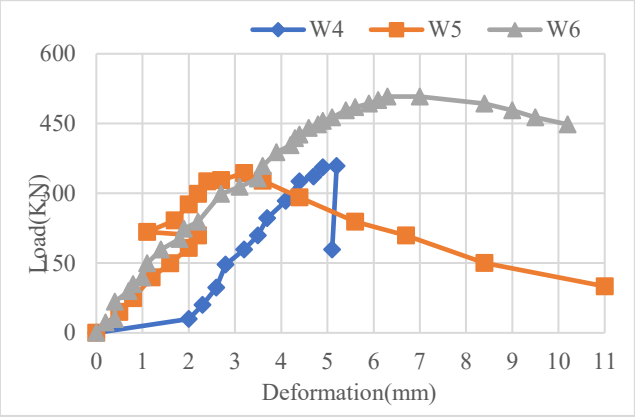

Figure 8. Load-Deflection of Group 2

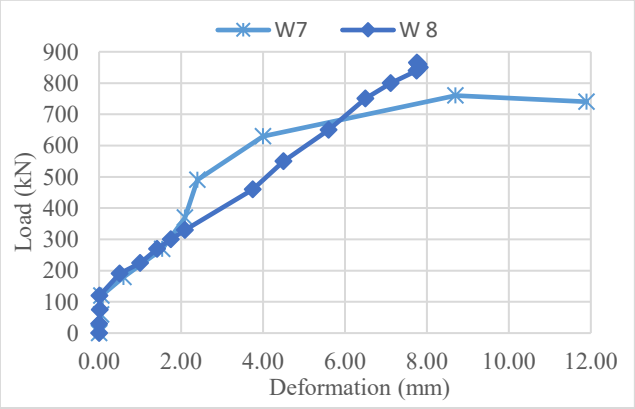

Figure 9. Deformation of Group 3.

4. Conclusion

In this work, eight AAC walls were tested by considering block height, mortar, and plastering materials as experimental variables. Cracking and failure loads were monitored and recorded together with modes of failure, strains, and deformations of walls. The main conclusions of these results were that the values of cracking and failure loads showed that AAC blocks were suitable for constructing load-bearing walls in comparison with the design of live and dead loads. According to the approved load codes, including the ASCE-7, the distributed live design loads on the floors do not exceed 5 kN/m2 for residential buildings, and approximately the same value is added to the dead design loads. By calculating the total loads falling on the walls, it is clear that the resistance of the walls made of AAC blocks is adequate to bear the service and design loads up to a safe and acceptable limit. Also, increasing of wall height as a result of decreasing the block height, showed an improvement in the strength of the wall because the mortar layers were increased and in turn reduced the formation and growth of cracks in the AAC layers, which enhanced the strength of the wall and the decrease in the thickness of the AAC blocks reduced the formation and growth of vertical and inclined cracks in the AAC layers, and the mortar began to act as barriers for these cracks, which led to an improvement load-bearing capacity. The results showed the adhesive mortar had a great adhesion strength, which increased the cohesion of the AAC blocks and improved the bearing capacity of the wall, which led to reduced deformation. The plastering of the wall affected the bearing strength by increasing the surface tensile bonds in the wall face, which contributed to improving the behavior of the wall and preventing or delaying the occurrence of cracks and fractures in the AAC blocks. Increasing the deformation depends on decreasing the block height, which decreases the layers of mortar, and also using cement-sand mortar because of its high resistance

to deformations that are transmitted to the AAC. Adding a reinforcement layer in the wall plastering had a significant effect on increasing the rigidity of the wall and decreasing the deformation. Finally, improving the resistance of the plastering layer by placing a steel wire mesh led to improving the stiffness and strength of the wall. The authors suggest conducting future studies of walls under eccentric loads, in addition to testing other elements of the AAC members in different dimensions, such as walls or beams under static and dynamic loads. It is also possible to review and evaluate design equations based on a relatively large number of specimens.

Conflict of Interest

The authors declare that there are no conflicts of interest regarding the publication of this manuscript.

Author Contribution Statement

Sarra'a Dhiya'a Jaafer carried out the experiments, discussed the experimental and theoretical results, formulated the F.E models, designed the tables and figures, and wrote the manuscript.

Ashraf A. Alfeehan was involved in planning and supervised the work, contributed to the interpretation of the results, and to the final writing of the manuscript.

Acknowledgments

The authors would like to thank Mustansiriyah University, Baghdad, Iraq, https://www.uomustansiriyah.edu.iq, for its support in the present work.

References

[1] G.-Q. Li and Y.-S. Liu, "Behavior of Steel Frames with and without AAC Infilled Walls Subjected to Static and Cyclic Horizontal Loads," in Proceedings of the 13th World Conference on Earthquake Engineering, Vancouver, BC, Canada, Aug. 1–6, 2004, Paper No. 1112, pp. 1–14. [Online].Available:https://www.iitk.ac.in/nicee/wcee/article/13_1112.pdf .

[2] R. R. Milanesi, P. Morandi, and G. Magenes, "Local effects on RC frames induced by AAC masonry infills through FEM simulation of in-plane tests," *Bull. Earthquake. Eng.*, vol. 16, no. 9, pp. 4053–4080, 2018. doi: https://doi.org/10.1007/s10518-018-0353-5.

[3] S. Bose and D. Rai, "Behavior of RC Frame Infilled with Low-Strength AAC Blocks," in Proceedings of the 12th North American Masonry Conference, Denver, CO, USA, May 17–20, 2015, pp. 1403–1414. [Online].Available: https://www.academia.edu/74639848/Behavior_of_RC_Frame_Infilled_with_Low_Strength_AAC_Blocks

[4] M. Basil, C. Sam-Amobi, C. C. Ugwu, and P. E. Odoh, "Combating global warming/climate change via reduction of CO2 emission of buildings," *IOPConf. Ser. Mater. Sci. Eng.*, vol. 640, no. 1, pp. 1–6, 2019. doi: 10.1088/1757-899X/640/1/012016.

[5] M. Deyazada, B. Vandoren, D. Dragan, and H. Degée, "Experimental investigations on the resistance of masonry walls with AAC thermal break layer," *Constr. Build. Mater.*, vol. 224, pp. 474–492, 2019. doi: https://doi.org/10.1016/j.conbuildmat.2019.06.205 .

[6] A. M. Saad, C. Gorse, C. I. Goodier, K. Blay, and S. Cavalaro, "Autoclaved Aerated Concrete in Reinforced Building Applications: a Systematic Review of AAC/RAAC in the Last 40+ Years," Results in Engineering, vol. 24, pp. 103431–103431, Nov. 2024. doi: https://doi.org/10.1016/j.rineng.2024.103431 .

[7] V. Kočí, J. Výborný, and R. Černý, "Computational and Experimental Characterization of Building Envelopes Based on Autoclaved Aerated Concrete," WIT Transactions on Engineering Sciences, vol. 72, pp. 363–373, 2011. doi: https://doi.org/10.2495/MC110321.

[8] M. Alaei, S. Mirvalad, and G. Pachideh, "Investigating the Characteristics of Autoclaved Aerated Concrete Containing Waste Materials," Case Studies in Construction Materials, vol. 23, p. e05058, Dec. 2025. doi: https://doi.org/10.1016/j.cscm.2025.e05058.

[9] S. Constantinescu, "Study on the Behavior of a High Reinforced Concrete Building with Different Kinds of Partitioning Masonry Walls," IOP Conference Series: Earth and Environmental Science, vol. 664, no. 1, p. 012050, 2021. doi: https://doi.org/10.1088/1755-1315/664/1/012050.

[10] L. Chen et al., "Green Construction Strategies to Combat Climate Change and Public-Health Issues," Cell Reports Physical Science, vol. 7, no. 1, pp. 103044–103044, Jan. 2026. doi: https://doi.org/10.1016/j.xcrp.2025.103044.

[11] T. Kothapally, U. Patil, C. Mounika, G. M. Naidu, G. K. B, and E. V. Kotov, "Experimental investigation on strength characteristics of autoclave aerated concrete block using natural pozzolanas," MATEC Web of Conferences, vol. 392, p. 01005, 2024. doi: https://doi.org/10.1051/matecconf/202439201005.

[12] R. Kumar, A. Thakur, and A. K. Tiwary, "A comparative study on conventional clay bricks and autoclaved aerated concrete blocks," *IOP Conf. Ser. Earth Environ. Sci.*, vol. 889, no. 1, p. 012061, 2021. doi: 10.1088/1755-1315/889/1/012061.

[13] O. F. Halici, U. Demir, Y. Zabbar, A. Ilki, and R. Klingner, "From experiments to seismic design rules for structures built with reinforced autoclaved aerated concrete panels," *Ce/Papers*, vol. 2, no. 4, pp. 275–282, Sep. 2018. doi: https://doi.org/10.1002/cepa.831.

[14] S. Constantinescu, "Adding a Masonry Floor on Top of a Reinforced Concrete High Building in a Seismic Area," IOP Conference Series: Materials Science and Engineering, vol. 789, no. 1, p. 012013, Mar. 2020. doi: https://doi.org/10.1088/1757-899x/789/1/012013.

[15] E. D. Khanal, A. P. D. A. K. Mishra, and A. P. B. Ghimire, "Technical suitability assessment of autoclaved aerated concrete block as alternative building wall construction material: A case of Nepal," *Saudi J. Civ. Eng.*, vol. 4, no. 5, pp. 55–67, 2020. doi: https://saudijournals.com/articles/946/

[16] J. Yu and Q. Sun, "Research on the failure feature of AAC load-bearing block wall based on the quasi-static test," *Adv. Mater. Res.*, vols. 287–290, pp. 1121–1124, 2011. doi: https://doi.org/10.4028/www.scientific.net/AMR.287-290.1121.

[17] J. Yu and S. Wu, "Experimental Study on Ductility and Dissipative Capacity of AAC Block Load-Bearing Walls," Applied Mechanics and Materials, vols. 90–93, pp. 1096–1099, 2011. doi: https://doi.org/10.4028/www.scientific.net/AMM.90-93.1096.

[18] A. Bhosale, N. P. Zade, R. Davis, and P. Sarkar, "Experimental investigation of autoclaved aerated concrete masonry," *J. Mater. Civ. Eng.*, vol. 31, no. 7, p. 04019109, 2019. doi: https://doi.org/10.1061/(ASCE)MT.1943-5533.0002762.

[19] R. Ayed et al., "Experimental and Computational Assessment of Building Structures Reinforced with Textile Fiber Waste to Improve Thermo-Mechanical Performance," Buildings, vol. 15, no. 3, p. 425, 2025. doi: https://doi.org/10.3390/buildings15030425.

[20] Borah, H. B. Kaushik, and V. Singhal, "Analysis and Design of Confined Masonry Structures: Review and Future Research Directions," *Buildings*, vol. 13, no. 5, pp. 1282–1282, 2023. doi: https://doi.org/10.3390/buildings13051282.

[21] U. A. Siddiqui, "Pseudo-dynamic testing and analytical modeling of AAC infilled RC frames," *J. Earthq. Eng.*, pp. 1281–1301, 2015. doi: https://doi.org/10.1080/13632469.2014.932723

[22] Ł. Drobiec and T. Rybarczyk, "Influence of reinforced concrete confining on the load-bearing capacity of the AAC walls," *Ce/Papers*, vol. 2, no. 4, pp. 409–415, 2018. doi: https://doi.org/10.1002/cepa.847

[23] M. S. Rasheed, "Analysis of reinforced concrete columns confined with fiber-reinforced polymer composites," M.Sc. thesis, Dept. Civ. Eng., Mustansiriya Univ., Baghdad, Iraq, 2017.

[24] S. H. Basha, Z. Guo, and X. Xie, "Effect of structural bonding patterns on mechanical characteristics of clay brick masonry under different loadings using digital image correlation technique," *J. Mater. Civ. Eng.*, vol. 34, no. 11, pp. 1–20, 2022. doi: https://doi.org/10.1061/(ASCE)MT.1943-5533.0004457